Complete Freund's Adjuvant-free experimental autoimmune encephalomyelitis in Dark Agouti rats is a valuable tool for multiple sclerosis studies

Milica Lazarević[a], Neda Djedovic[a], Suzana Stanisavljević[a], Mirjana Dimitrijević[a], Goran Stegnjaić[a], Gurumoorthy Krishnamoorthy[b], Marija Mostarica Stojković[c], Đorđe Miljković*[a], Bojan Jevtić[a]

[a]Department of Immunology, Institute for Biological Research "Siniša Stanković" - National Institute of Republic of Serbia, University of Belgrade, Despota Stefana 142, 11000 Belgrade, Serbia

[b]Max Planck Institute of Biochemistry, Am Klopferspitz 18, 82152 Martinsried

[c]Institute of Microbiology and Immunology, School of Medicine, University of Belgrade, Dr Subotića 1, 11000 Belgrade, Serbia

[*]Corresponding author:

Đorđe Miljković, PhD

Department of Immunology

Institute for Biological Research "Siniša Stanković" - National Institute of Republic of Serbia, University of Belgrade

Despota Stefana 142, 11000 Belgrade, Serbia

Tel: +381 11 2078390

E-mail: georgije_zw@yahoo.com

Abstract

Experimental autoimmune encephalomyelitis (EAE) is classically induced with complete Freund's adjuvant (CFA). The immune response against CFA has a confounding influence on the translational capacity of EAE as a multiple sclerosis model. Here, we compare clinical, cellular and molecular properties between syngeneic spinal cord homogenate (SCH)- and SCH+CFA-immunized Dark Agouti rats. EAE signs were observed earlier and the cumulative clinical score was higher without CFA. Also, a higher number of immune cells infiltrates in the spinal cords was noticed at the peak of EAE without CFA. High spinal cord abundance of $CD8^+CD11bc^+MHCclassII^+$ was detected in SCH-immunized rats. Myelin basic protein -specific response can be elicited in the cells from the lymph nodes draining the site of SCH immunization. This CFA-free EAE is a reliable multiple sclerosis model.

Keywords

EAE; CFA; $CD4^+$ T cells; $CD8^+$ macrophages.

Abbreviations

CFA: Complete Freund's Adjuvant; CNS: Central nervous system; d.p.i.: day post-immunization; EAE: Experimental autoimmune encephalomyelitis; MBP: Myelin basic protein; MFI: Mean fluorescent intensity; MS: Multiple sclerosis; PBS: Phosphate buffered saline; PLN: Popliteal lymph node; PLNC: Popliteal lymph node cells; SCH: Spinal cord homogenate.

1. Introduction

Multiple sclerosis (MS) is a chronic inflammatory, demyelinating and neurodegenerative disease of the central nervous system (CNS). Experimental autoimmune encephalomyelitis (EAE) has been traditionally considered as a valuable animal model for multiple sclerosis-related studies (Ben-Nun et al., 2014). Although there are several models of EAE, none of them is without caveats (Sriram and Steiner, 2005). Mice EAE models have been dominating multiple sclerosis research over the past 40 years (Burrows et al., 2019; Croxford et al., 2011). The main reasons are the smaller size and lower price of mice in comparison to rats and other laboratory animals, thus higher numbers of mice for the experiments can be afforded. Furthermore, many more species-specific reagents, including antibodies are generated for mice than for rats. Finally, genetic modification of mice, but not rats is common and there are many mice lines defective for or overproducing immune molecules. On the other hand, rats are larger, isolation and analysis of their spinal cord, brain and lymph nodes is easier, and they can be used in intravital imaging easier than mice (Croxford et al., 2011). Also, in most of the mice, but not rat strains use of pertussis toxin (PT) is essential for EAE induction (Burrows et al., 2019). One common species-unspecific limitation is that EAE immunization relies on the use of CFA which is mixed with the CNS proteins to form the encephalitogenic emulsion. CFA contains killed *Mycobacteria* and various pathogen-associated molecular patterns contribute to the efficient initiation of the autoimmune response in EAE (Mills, 2011). There are several concerns regarding the use of CFA as the adjuvant in EAE. CFA stimulates the immune response against non-CNS antigens on its own, *i.e.* strong anti-purified protein derivative response is induced, regardless of the CNS autoantigens (Namer et al., 1993). It skews the immune response towards Th1-driven response (Billiau and Matthys, 2001), thus interfering with the study of other cell populations involved in

neuroinflammation. CFA induces pain by itself, paralleled with activation of glia and production of inflammatory mediators in the spinal cord (Raghavendra et al., 2004). Since immunization with CFA represents a standard model for studying pain (Coderre and Laferrière, 2020), EAE induced with CFA is not a reliable animal model for analyzing the mechanism underlying chronic neuropathic pain frequently registered in MS patients (Solaro et al., 2013). Biochemical changes, as well as differential gene expression profiles in the CNS of animals in which EAE was induced by immunization with CFA (Ibrahim et al., 2001) might be at least partially ascribed to adjuvant alone (Chu et al., 2005). The use of CFA containing or supplemented with different types of *Mycobacterium* species, e.g. *M. tuberculosis* and *M. butyricum* may influence the reproducibility of EAE results (Laman et al., 2017). Therefore, CFA is a confounding element that impedes translation of the results of EAE studies for the benefit of multiple sclerosis patients. There have been attempts to eliminate CFA from the immunization protocol in EAE. Substitution of CFA with incomplete Freund's adjuvant which lacks *Mycobacteria*, supposed to be responsible for effects mentioned above, has been shown unpractical in mice where it provoked tolerance (Mills, 2011). This substitution was efficacious in rats (Paterson and Bell, 1962) and some primates (Haanstra et al., 2013; Jagessar et al., 2012) but there is no successful known disease induction without CFA in mouse models. Our group has been successful in eliminating adjuvant in Dark Agouti (DA) rats, where reliable EAE can be induced with rat spinal cord homogenate (SCH) only (Stosic-Grujicic et al., 2004).

In this study, we compare CFA-free EAE, to a classical EAE in DA rats to evaluate CFA-free EAE as a more reliable model exhibiting crucial features of MS and devoid of all confounding effects of CFA. We have focused on the clinical course, spinal cord pathological findings, and on

detailed phenotyping of the immune cells in the lymph nodes draining the site of immunization, in the blood, and within the CNS.

2. Material and methods

2.1. Experimental animals and EAE

DA rats were bred and maintained in the animal facility of the Institute for Biological Research "Sinisa Stankovic". Animal experiments were approved by the Veterinary Administration, Ministry of Agriculture, Forestry and Water Management, Republic of Serbia (№ 323-07-01337/2020-05). Five to seven months old rats of both sexes were used in experiments. The housing of the rats was performed under controlled environmental conditions. Three to five rats were kept in the same cage. Two ways of immunization were performed: DA rat SCH in phosphate buffered saline (PBS, 50% w/v) – SCH-immunized rats, and DA rat SCH in PBS (50% w/v) mixed with an equal volume of complete Freund's adjuvant (CFA, Difco, Detroit, MI) supplemented with 5 mg/ml of *M. tuberculosis* H37Ra (Difco) – SCH+CFA-immunized rats. The animals were injected subcutaneously into hind limbs with 200 μL of SCH homogenate in PBS or 150 μL of SCH+CFA emulsion. PT was not applied to rats, irrespectively of the immunization. The rats were monitored daily for clinical signs of EAE, and scored according to the following scale: 0, no clinical signs; 1, flaccid tail; 2, hind limb paresis; 3, hind limb paralysis; 4, moribund state or death. Cumulative clinical score was calculated as a sum of daily clinical scores, Mean clinical score was calculated as cumulative clinical scores divided by the duration. To detect inflammatory infiltrates in the CNS of immunized animals, hematoxylin and eosin staining was performed on spinal cord tissue sections from 5 animals. Infiltrates were defined as the clusters of mononuclear cells localized in the perivascular space and the subpial region of the spinal cord. Five micrometers of transversal lumbosacral sections (L1 – L5) were cut and 8 successive slices were placed on the same glass slide. The number of infiltrates and cells per infiltrate were counted from 120 spinal cord tissue sections per group, as described

previously (Stanisavljević et al., 2019). To detect demyelinating regions in the spinal cord sections, Sudan black staining was performed as described previously (Lavrnja et al., 2017). In brief, paraffin spinal cord sections were rinsed with propylene glycol and stained for 10 min with 0.7 % Sudan black B (Sigma-Aldrich, St. Louis, MO, USA) diluted in propylene glycol.

2.2. Isolation of cells, cell culture, and generation of supernatants

Cells of lymph nodes draining the site of immunization (popliteal lymph nodes, PLN) were obtained from immunized rats at day 4 and day 6 post-immunization (p.i.). Inguinal lymph nodes were isolated in addition to popliteal lymph nodes from non-immunized rats, age and sex matched to the immunized ones. PLN cells (PLNC) were obtained by mechanical disruption. The cells were seeded at 5 x 10^6/ml/well in 24-well plates (Sarstedt, Nümbrecht, Germany) and stimulated with MBP (10 μg/ml, guinea pig MBP, a kind gift from Professor Alexander Flügel, University of Göttingen, Germany). The cells were grown in RPMI1640 medium supplemented with 2% rat serum. Cultures lasted for 24 h and subsequently cell culture supernatants were collected and kept frozen until assayed. Spinal cord immune cells were isolated from the immunized rats. Rats were extensively perfused with cold PBS before spinal cord isolation. Spinal cords were homogenized and homogenates were centrifuged using a 30/70% gradient of Percoll (Sigma-Aldrich). Following centrifugation, immune cells were recovered from the Percoll interface and washed in RPMI medium.

2.3. Cytofluorimetry

Cells were stained with the following antibodies: biotin-conjugated anti-CD3 (mouse monoclonal G4.18, BD Pharmingen, San Jose, CA, USA), FITC-conjugated anti-CD3 (mouse monoclonal G4.18, eBioscience, San Diego, CA, USA), biotin-conjugated anti-CD4 (mouse

monoclonal OX35, BD Pharmingen), FITC- or PE-conjugated anti-CD4 (mouse monoclonal OX35, eBioscience), biotin-conjugated anti-CD8a (mouse monoclonal OX8, BD Pharmingen), FITC- or PE-conjugated anti-CD8a (mouse monoclonal OX8, eBioscience), PE-conjugated anti-CD25 (mouse monoclonal OX39, eBioscience), FITC-conjugated anti-CD45 (mouse monoclonal OX1, eBioscience), PE-conjugated anti-CD11bc (mouse monoclonal OX42, eBioscience), FITC-conjugated anti-MHCclassII (mouse monoclonal 14-4-4S, eBioscience), PE-conjugated anti-MHCclassII (mouse monoclonal HIS19, eBioscience), FITC-conjugated anti-CD45RA (mouse monoclonal OX33, Invitrogen, Carlsbad, CA, USA), FITC-conjugated anti-granulocyte marker (mouse monoclonal HIS48, eBioscience), PE-conjugated anti-CD314 (mouse monoclonal 11D5F4, eBioscience), biotin-conjugated anti-CD134 (mouse monoclonal OX40, BD Pharmingen), PE-conjugated anti-IL-10 (mouse monoclonal A5-4, BD Pharmingen), PerCP-Cy5.5-conjugated anti-IL-17 (rat monoclonal eBio17B7, BD Pharmingen), biotin-conjugated anti-IFN-γ (rabbit polyclonal, eBioscience), and PerCP-Cy5.5-conjugated anti-Foxp3 (rat monoclonal FJK-16s, eBioscience). Biotin-conjugated antibodies were detected with PECy5-conjugated streptavidin (Biolegend, San Diego, CA, USA). Intracellular staining for cytokines and FoxP3 were performed according to the procedure suggested by the manufacturer (eBioscience), using Foxp3 / Transcription Factor Fixation/Permeabilization Concentrate and Diluent, Intracellular Fixation & Permeabilization Buffer Set, and Permeabilization Buffer (all from eBioscience), as appropriate. Adequate isotype control antibodies were used where necessary to set gates for cell marker positivity. Typically, the proportion of isotype control antibody-stained cells was <1%. The gating strategy is presented in Supplementary Fig1. The acquisition of the samples was performed on a Partec CyFlow Space cytometer (Partec, Munster, Germany) and analyzed by FloMax software (Partec). Results of cytofluorimetry are presented

as the proportion of cells bound by an appropriate antibody or by mean fluorescent intensity (MFI) per cell.

2.4. ELISA

Cytokine concentration in cell culture supernatants was determined by sandwich ELISA using MaxiSorp plates (Nunc, Rochild, Denmark). For IFN-γ and IL-17 detection anti-cytokine paired antibodies were used according to the manufacturer's instructions (eBioscience). The antibodies were as follows: anti-rat IFN-γ purified mouse monoclonal (DB1), anti-rat IFN-γ biotinylated rabbit polyclonal, anti-mouse/rat IL-17A purified rat monoclonal (eBio17CK15A5) and anti-mouse/rat IL-17A biotinylated rat monoclonal (eBio17B7). Samples were analyzed in duplicates and the results were calculated using standard curves based on known concentrations of the recombinant rat IL-10 (R&D Systems) and IFN-γ and IL-17 (Peprotech, Rocky Hill, NJ).

2.5. Statistical analysis

The significance of the differences between the groups was determined using a two-tailed Student's t-test, Mann-Whitney U test, and one-way ANOVA or two-way ANOVA (factors: immunization x culturing condition) followed by Tukey's post hoc test where appropriate. A p value less than 0.05 was considered statistically significant.

3. Results

3.1. Clinical course of EAE in rats immunized without or with CFA

EAE clinical signs in SCH-immunized DA rats were followed for 35 days. Results obtained with male and female rats were compared to determine if there were some sex differences in the susceptibility and the clinical course of EAE (Fig 1A). The incidence of EAE was 100% in male rats (12/12) and 91.7% in female rats (11/12). Although there was a trend for earlier initial clinical signs and higher values of cumulative, mean, and maximal clinical scores in female rats, none of the differences reached the level of statistical significance (Table 1). The EAE clinical course was also analyzed in a comparative study of age and sex-matched DA rats immunized with SCH or with SCH+CFA and monitored for 18 days after the immunization (Fig 1B). EAE symptoms were observed in 42 out of 45 SCH-immunized rats and in 39 out of 40 SCH+CFA-immunized rats (93.3% and 97.5% of incidence, respectively). Initial clinical signs of EAE were observed in SCH-immunized rats approximately one day before the onset in SCH+CFA-immunized rats (Table 2). Cumulative clinical scores were higher in SCH-immunized rats (Table 2). Duration, mean clinical scores and maximal clinical scores were not different between the two groups of rats. Histological screening of the spinal cords at the peak of EAE (clinical scores 2.5 or 3) showed that the number of infiltrates in the whole spinal cords, as well as in the white matter was slightly, but significantly higher in SCH-immunized rats, while there was no difference in the number of infiltrates in the gray matter between the groups (Fig 1C, D). The number of cells per infiltrate was without the difference between the groups irrespectively of their localization (Fig 1E). Demyelination was present in spinal cords of rats at the peak of EAE, irrespectively of the immunization protocol (Fig 1F).

Table 1. Comparison of EAE clinical parameters in male and female SCH-immunized rats in 35 day follow up.

	n	onset (days)	cumulative clinical score	duration (days)	mean clinical score	max clinical score
Male	12	9.0 +/- 1.2	30.0 +/- 10.6	18.8 +/- 7.3	1.8 +/- 0.8	3.0 +/- 0.9
Female	11	8.2 +/- 1.0	34.3 +/- 9.7	16.5 +/- 8.5	2.3 +/- 0.6	3.5 +/- 0.4

Table 2. EAE clinical parameters in SCH- and SCH-CFA- immunized rats in 18 days follow-up.

	n	onset (days)	cumulative clinical score	duration (days)	mean clinical score	max clinical score
SCH	42	9.5 +/- 0.3	16.4 +/- 1.5	8.1 +/- 0.5	1.9 +/- 0.1	2.5 +/- 0.2
SCH+CFA	39	10.2 +/- 0.3*	11.4 +/- 0.8*	7.3 +/- 0.3	1.6 +/- 0.1	2.6 +/- 0.1

*$p<0.05$ SCH *vs.* SCH+CFA

3.2. Immune cell populations in the lymph nodes draining the site of immunization

Immune cells were isolated from PLN draining the site of immunization at day 4 and day 6 p.i. with SCH or SCH+CFA. Also, popliteal and inguinal lymph nodes were isolated from non-immunized rats. Inguinal lymph nodes were included, as popliteal lymph nodes are small with an insufficient number of cells in non-immunized rats. The number of cells isolated from the lymph nodes was lower in SCH-immunized rats than in SCH+CFA-immunized rats at day 4 and day 6 p.i. (Fig 2A). In comparison to lymph nodes of non-immunized rats, the percentage of $CD4^+$ T

cells was lower PLN of rats immunized in either of the ways (Fig 2B). The proportion of $CD4^+$ T cells was also significantly lower in SCH- than in SCH+CFA-immunized rats (Fig 2B) at both time points. The proportion of $CD8^+$, $CD11bc^+$, and $CD45RA^+$ cells (B cells) was higher in immunized than in non-immunized rats, while the percentage of MHC class II^+ cells was without a difference (Fig 2C-F). There was no difference in the proportion of $CD8^+$, $CD11bc^+$, MHC class II^+ or $CD45RA^+$ (B cells) in the lymph nodes of SCH- and SCH+CFA-immunized rats (Fig 2C-F). The absolute number of $CD4^+$, $CD8^+$, $CD11bc^+$, MHC class II^+, and $CD45RA^+$ cells was lower in SCH -immunized rats at day 4 p.i. (Fig 2G-K). At day 6 p.i., the number of $CD4^+$ and $CD8^+$ was also lower in SCH-immunized rats (Fig 2G, H). The proportion of $CD4^+$ T cells expressing OX40, *i.e.* activated $CD4^+$ T cells was higher in immunized than in non-immunized rats (Fig 2 L). However, there was no increase in $OX40^+$ cells among $CD8^+$ T cells in the immunized rats (Fig 2M). Proportion and absolute number of $CD4^+$ and $CD8^+$ T cells expressing OX40 were lower in SCH- than in SCH+CFA-immunized rats at day 4 p.i. (Fig 2L-O). However, on day 6 p.i., only the absolute number of $OX40^+CD8^+$ cells was lower in SCH-immunized rats (Fig 2O). Further, the proportion of CD4 T cells expressing CD25 increased in the immunized rat PLN (Fig 2P). The absolute number of $CD25^+CD4^+$ T cells, but not the proportion of $CD25^+$ cells among $CD4^+$ T cells, was lower in SCH- than in SCH+CFA-immunized rats at both time points (Fig 2P, Q). IL-17-, IFN-γ– and IL-10-producing cells were determined among $CD4^+$ and $CD8^+$ T cells of non-immunized and immunized rats (Fig 2R-AC). The proportion of the cytokines-expressing T cells was low in non-immunized rats in comparison to the immunized ones (Fig2 R-W). Both SCH and SCH+CFA immunization led to an increase in the proportion of T cells expressing the cytokines, except for IL-17 in CD8 T cells (Fig 2 R-W). There were no statistically significant differences in the proportion of T cells expressing the cytokines between

SCH- and SCH+CFA-immunized rats, except for IL-10-expressing $CD4^+$ T cells at day 4 p.i. (Fig 2R-V). Also, the production of cytokines per cell was similar in PLN T cells of differently immunized rats as judged by MFI for cytokines expression in $CD4^+$ and $CD8^+$ T cells (data not shown). However, absolute numbers of T cells expressing IL-17, IFN-γ and IL-10 were statistically significantly lower in SCH-immunized rats on day 4 and day 6 p.i., except for IL-17-expressing $CD8^+$ T cells at day 6 p.i. (Fig 2X-AC). Finally, both immunizations led to an increase in the proportion of $CD4^+CD25^+FoxP3^+$ Treg in comparison to non-immunized rats, while there was no difference in the percentage of Treg among $CD4^+$ PLNC between SCH and SCH+CFA-immunized rats (Fig 2AD). Absolute numbers of Treg were lower in $CD4^+$ PLNC of SCH- immunized rats (Fig 2AE). Thus, both immunizations induced strong activation of $CD4^+$ T cells and limited activation of $CD8^+$ T cells in PLN. Also, PLN of SCH-immunized rats had a lower total cell number, number and proportion of $CD4^+$ T cells and activated $CD4^+$ T cells than those of SCH+CFA-immunized rats at the initiation of an immune response. Finally, the lower absolute number of cytokine-producing T cells was observed in SCH-immunized rats than in SCH+CFA-immunized counterparts.

3.3. Response of the PLNC to MBP stimulation

To determine whether CFA influences the activation of MBP-specific cells and their capacity to produce IL-17 and IFN-γ, PLNC were isolated from SCH- and SCH-CFA-immunized rats in the inductive phase of EAE and incubated with MBP (10 μg/ml) for 24 hours. Higher basal production of IL-17 was observed in SCH+CFA samples (Fig 3A). The rise of both cytokines levels was detected in the cell culture supernatants in response to MBP both in SCH- and SCH-CFA-immunized rats (Fig 3). The increase in the release of the cytokines in PLNC in response to

MBP was markedly higher in rats immunized with SCH only (Fig 3). The increase of IL-17 production was 29.3 folds and 4.7 folds in SCH and SCH+CFA samples, respectively. The increase of IFN-γ production was 33.7 folds and 15.3 folds in SCH and SCH+CFA samples, respectively (Fig 3B). Therefore, although the absolute number of IFN-γ– and IL-17-expressing cells was lower in PLNC of SCH immunized rats (Fig 2X-AC), *in vitro* stimulation with MBP induced equal production of IL-17 and significantly higher production of IFN-γ in SCH-immunized rats. These results suggest that immunization with CFA is inferior in the expansion of MBP-specific cells capable of producing EAE pathogenic cytokines, probably due to their lower frequency in PLNC of SCH+CFA-immunized rats.

3.4. Analysis of the spinal cord immune cells isolated at the peak of EAE

Immune cells were isolated from the spinal cord of rats at the peak of EAE. Rats from both immunization groups were sacrificed at the time of the peak of the disease (clinical score 2.5-3.5, day 3 or day 4 after the initial symptoms were observed). The number of cells isolated from the spinal cords was without the difference between the groups (Fig 4A). The proportion of $CD4^+$ cells among immune cells isolated from the spinal cord was similar in SCH- and SCH-CFA immunized rats (Fig 4B). The proportion of $CD8^+$ cells was higher, while that of $CD3^+$ cells was lower in SCH-immunized rats (Fig 4B). The proportion of $CD4^+$ cells among $CD3^+$ cells *i.e.* T cells was similar in both groups (Fig 4C). However, the proportion of $CD8^+$ T cells was lower in SCH-immunized rats (Fig 4C). The proportion of activated $CD8^+$ T cells, *i.e.* $CD25^+$ or $OX40^+$ cells was lower in SCH-immunized rats, while the proportion of activated $CD4^+$ T cells was similar in both immunization groups (Fig 4D, E). The proportion of cells infiltrating from the blood ($CD45^+$) was similar between the groups (Fig 4F), as well as the percentage of $CD11bc^+$ cells (macrophages, microglia, NK cells, granulocytes, dendritic cells). Also, the proportion of

inactive microglia (CD11bc^{+}CD45-) was similar between the groups (Fig 4G). These results show subtle differences in the composition of the CNS infiltrates at the peak of EAE between the immunizations.

3.5. Phenotypic characterization of spinal cord immune cells in SCH-immunized rats

Immune cells were isolated from spinal cords of SCH-immunized rats at the onset (clinical scores 1, duration 1 day), at the peak (clinical scores 3, duration 3 or 4 days), and the recovery (clinical scores 1, duration 12 or 13 days). There was a trend of an increase in the number of cells isolated from the spinal cord from the onset to the recovery (Fig 5A). The proportion of T cells (CD3^{+} cells) was low at the onset, increased at the peak, and slightly decreased towards the recovery (Fig 5B). The majority of T cells were CD8^{+} cells at the onset, followed by CD4^{+} cells, CD314^{+}, *i.e.* NKT cells, and CD4^{+}CD8^{+} cells (Fig 5B). However, CD4^{+} cells were the most abundant among T cells at the peak and the recovery. The proportion of CD8^{+} cells among T cells decreased at the peak, and the recovery. The proportion of NKT cells among T cells was without a significant difference among the examined time points. Interestingly, the proportion of CD4^{+}CD8^{+} T cells increased significantly at the recovery, in comparison to either of the previous time points. The proportion of CD4^{+} and CD8^{+} cells that were OX40 positive was rather stable throughout the observation period within the CNS (Fig 5C). Less than 1% of either CD4^{+} T cells or CD8^{+} T cells expressed activation marker OX40 in the blood at the onset, peak, and recovery (data not shown). The proportion of CD314^{+} cells, *i.e.* NK cells increased from the onset to the peak and stayed at the same level at the recovery (Fig 5D). The majority of CD314^{+} cells were CD3-expressing cells, *i.e.* NKT cells throughout the examination period. Granulocytes (His48^{med}CD11bc^{high}) were abundant at the onset and then declined at the peak, and they were almost undetectable at the recovery (Fig 5E). The proportion of B cells (CD45RA^{+}) was low

throughout the observation period (Fig 5E). $CD11bc^+$ dominated at the onset and the peak, while their proportion was lower than 50% at the peak of EAE (Fig 5F). Inactive microglial cells ($CD11bc^+CD45^-$) were more than a third of the total isolated cells at the onset and the recovery, but less than 10% at the peak (Fig 5F). Less than 30% of $CD11bc^+$ cells expressed MHC class II molecules at the onset of EAE, but the proportion of $CD11bc^+$ cells expressing MHC class II molecules rose to more than 90% at the recovery (Fig 5F). MHC class II positive cells rose from the onset to the peak and then to the recovery when they were more than 60 % of the cells (Fig 5G). Most of the MHC class II positive cells were $CD11bc^+$ cells, while B cells contributed less than 5% of the MHC class II positive population. $CD8^+CD11bc^+$ cells (macrophages) were less than 4% at the onset, increased at the peak to over 10% of the total cells, and then slightly decreased at the recovery (Fig 5H). Importantly, more than half of these cells were also MHC class II^+ already at the onset, while the proportion of MHC class II^+ cells among $CD8^+CD11bc^+$ cells was more than 85 % at the peak and then decreased to the recovery (Fig 5H). Importantly, $CD8^+CD11bc^+$ monocytes in the blood had a minor proportion of those expressing MHC class II (Fig 5I), and the mean fluorescent intensity of the expression was much lower in the peripheral blood cells (Fig 5J). The mean fluorescence intensity of MHC class II expression in $CD8^+CD11bc^+$ cells in the CNS was the highest at the peak of EAE (Fig 5J). $CD4^+CD11bc^+$ (macrophages/activated microglia) proportion increased from the onset to the recovery (Fig 5K). Less than 30 % of these cells were positive to MHC class II at the onset, but the proportion was over 80% at the onset and more than 95% at the recovery (Fig 5K). $CD4^+CD11bc^+$ monocytes were present among peripheral blood mononuclear cells in proportion less than 10 % at any of the examined time points and only a minority of these cells expressed MHC class II molecules (Fig 5L). Also, the mean fluorescent intensity of MHC class II expression among blood

$CD4^+CD11bc^+$ cells was much lower than in the spinal cord (Fig 5M). CNS $CD4^+CD11bc^+$ cells also had the highest mean fluorescent intensity of MHC class II expression at the peak of EAE (Fig 5M). These results imply that both $CD8^+CD11bc^+$ and $CD4^+CD11bc^+$ cells are already present in the peripheral blood, but that only upon entering the CNS, they acquire the phenotypic characteristics of efficient antigen-presenting cells. Also, it seems that these two populations are among the major antigen-presenting cells in the inflamed CNS of SCH-immunized rats, with $CD8^+CD11bc^+$ cells being more potent at the onset of the disease.

4. Discussion

Our present study shows that EAE can be induced in DA rats without CFA using whole spinal cord homogenate (SCH). Clinical and histological manifestations of EAE are even more pronounced in DA rats immunized with SCH in the absence of CFA, although the response to the immunization, as judged by cellular proliferation in the lymph nodes draining the site of injection, seems weaker without CFA. Subtle differences in the composition of spinal cord immune cell infiltrates were observed in DA rats immunized with SCH only and SCH+CFA.

Several recent papers identified extensive heterogeneity of the cellular make-up in neuroinflammation by applying sophisticated techniques such as single-cell transcriptome analysis (Gaublomme et al., 2015; Jordão et al., 2019) and high-dimensional single-cell mass and fluorescence cytometry (Mrdjen et al., 2018). However, the obtained results are derived from the CNS of animals in which EAE was induced with the aid of CFA. Besides all previously mentioned confounding aspects of CFA, in the context of defining multiple immune cells in neuroinflammation, it is necessary to take into account the capacity of CFA to induce glial cell activation (Raghavendra et al., 2004) and increase blood-brain permeability (Brooks et al., 2005) by itself. Therefore, the model of EAE induced without CFA described in this report might provide better insight into the immune cells participating in EAE.

Despite the lower number and inferior activation of T cells in the lymph nodes draining the site of immunization in SCH-immunized DA rats in comparison to SCH+CFA-immunized counterparts, equal numbers of immune cells are retrieved from the spinal cord of EAE rats at the peak of the disease, regardless of the immunization. Moreover, a higher number of infiltrates is observed in SCH-immunized rats. These facts support the idea that CFA is activating T cells

on its own, but that homing and retention of T cells is superior without CFA. This might be the consequence of dilution of the CNS-specific T cells by T cells specific for mycobacterial constituents within CFA. Without CFA, the majority of cells proliferating in the lymph nodes draining the site of immunization are specific for the spinal cord antigens. Therefore, they will be able to recognize antigens once they arrive in the CNS and to be re-activated. With CFA, many activated T cells are not specific for the spinal cord antigens, but for mycobacterial antigens, and such cells will not receive adequate support within the CNS. Indeed, it was previously shown in a transfer EAE in rats that both MBP- and ovalbumin-specific cells invaded the CNS with similar efficiency, but that only former were properly re-activated within the CNS by the local antigen-presenting cells (Bartholomäus et al., 2009; Kawakami et al., 2005). The higher increase in the release of IL-17 and IFN-γ in response to MBP by the lymph node cells of SCH-immunized rats in comparison to SCH+CFA-immunized rats supports our assumption on the CFA-imposed dilution of the CNS specificity of the immune response. Importantly, the ability of the lymph node cells to produce IL-17 and IFN-γ in response to MBP also supports the possibility to generate MBP-specific $CD4^+$ T cell lines from these cells. This possibility is currently being explored in our laboratory with the idea to use such cell lines for the adoptive transfer of EAE. To the best of our knowledge, this transfer EAE model would be the first acquired without the use of CFA. Further, SCH immunization likely elicits T cell response to other CNS antigens, such as myelin oligodendrocyte glycoprotein (MOG) and myelin proteolipid protein (PLP). Indeed, the proliferative response of cells isolated from the lymph nodes draining the site of SCH immunization to MOG and PLP peptides was shown in the initial study (Stosic-Grujicic et al., 2004). Thus, further exploration of the antigen specificity elicited by SCH immunization in DA rats is warranted.

Besides inactive microglia, which accounted for one-third of all isolated cells from the spinal cord of SCH-immunized DA rats at the onset of EAE, $CD8^+$ cells and granulocytes dominated the infiltrates. Importantly, $CD8^+$ T cells dominated over $CD4^+$ T cells at the onset of EAE. This is of particular interest having in mind a growing body of evidence implying the importance of $CD8^+$ T cells in multiple sclerosis pathogenesis (Hohlfeld et al., 2016). Also, neutrophils have become increasingly appreciated as important players in EAE and multiple sclerosis induction (Pierson et al., 2018), but also in relapses and progression of multiple sclerosis (Casserly et al., 2017). In our previous work, neutrophils were identified as the dominant population in the fulminant EAE induced in DA rats (Miljković et al., 2011). However, macrophages seem to be of particular interest in the pathogenesis of EAE in SCH-immunized DA rats. Worth mentioning, macrophages were shown indispensable for SCH+CFA EAE induction in DA rats (Mensah-Brown et al., 2011). Here, we present that $CD8^+$ macrophages might be the dominant antigen-presenting cells in the CNS of SCH-immunized rats as deduced by their potent expression of MHC class II molecules, especially at the onset and at the peak of EAE. Also, a high abundance of $CD4^+$ macrophages/microglia expressing MHC class II molecules was observed in the CNS of SCH-immunized DA rats at the peak and recovery phase of the disease. Both, CD8- and CD4-expressing macrophages have been previously linked with CNS inflammation. $CD8^+$ macrophages were initially identified in the CNS in focal cerebral ischemia in rats (Jander et al., 1998), followed by the finding in the spinal cord injury model (Popovich et al., 2003). Also, they were observed in the peripheral nervous system, *i.e.* sciatic nerves of rats with crush nerve injury (Jander et al., 2001) and with experimental autoimmune neuritis (Zhang et al., 2016). They have already been identified in rat EAE, in MOG-induced chronic EAE, but not in MBP-induced acute EAE (Hiraki et al., 2009; Schroeter et al., 2003). In all of these models, they were linked to

tissue destruction. On the other hand, they have been associated with the limitation of the autoimmune response in glomerulonephritis in rats (Wu et al., 2014). Despite their increased abundance and their increased expression of MHC class II correlated with the peak of the disease in SCH-induced EAE, it would be necessary to perform further experiments to find out their exact role in the pathogenesis of the disease. $CD4^+$ expression on macrophages and microglia in the CNS has been known for a long time (Perry and Gordon, 1987). It was shown that macrophages/microglia express CD4 in the CNS during EAE, and it was suggested that $CD4^+$ microglia, defined as $CD11b^+CD45^{low/intermediate}$ cells, contributed to the recovery of rats from the disease (Almolda et al., 2009). The highest abundance of $CD4^+CD45^{high}CD11b^+$ cells, *i.e.* of activated macrophages/microglia was observed at the peak of EAE (Almolda et al., 2009). Our data show that majority of $CD4^+CD11bc^+$ cells express MHC class II molecules at the peak and the recovery, thus suggesting their prominent role in the interaction with $CD4^+$ T cells within the CNS in these phases of EAE. At this point, it is hard to tell if $CD4^+$ macrophages/microglia contribute to tissue destruction or the resolution of the inflammation in the CNS of EAE DA rats. Finally, $CD8^+$ and $CD4^+$ macrophages have been identified in humans as well (Gibbings and Befus, 2009; Gibbings et al., 2007; Herbein et al., 1995), but their role in multiple sclerosis is still elusive. Interestingly, $CD8^+$ and $CD4^+$ macrophages have not been identified in mice (Crocker et al., 1987; Gibbings and Befus, 2009) thus supporting the use of rat animal models in investigating human pathologies, including multiple sclerosis (Wildner, 2019).

Although B cells were scarce in the spinal cord of SCH-immunized rats their role in the CNS inflammation in our model can not be excluded. Having in mind that there is an increased interest in B cell contribution to the pathogenesis of multiple sclerosis and the therapeutic success of anti-CD20 therapy in relapsing-remitting and even primary progressive multiple

sclerosis (D'Amico et al., 2019; Hohlfeld et al., 2016) it is our goal to investigate B cell and antibody contribution to EAE pathogenesis in SCH-immunized DA rats in details in future. Also, NK and NKT cells are present in the spinal cord of SCH-immunized rats. It will be important to study their role in the disease pathogenesis, as well. This is particularly important having in mind recent findings on the induction of immunoregulatory NK cells by Daclizumab in multiple sclerosis patients (Mimpen et al., 2020). $CD4^+CD8^+$ double-positive T cells are also worthy of further studies in SCH-immunized DA rats, as they are enriched in the CNS at the recovery phase. In support of such a view, $CD4^+CD8^+$ T cells were previously shown effective in ameliorating EAE in mice (Tutaj and Szczepanik, 2007).

5. Conclusions

This comparative study clearly shows that CFA is a confounding factor in EAE, as it skews the autoimmune response both in immune organs and within the CNS. Our ongoing studies aim to determine if CFA in DA rats influences gut microbiota and gut immune cells that have been increasingly appreciated in EAE pathogenesis (van den Hoogen et al., 2017) and as previously shown in adjuvant-induced arthritis in SD rats (Pan et al., 2019). Our further studies will be directed towards functional characterization and modification of the cell populations identified as potentially important for the pathogenesis of SCH-induced EAE in DA rats, such as $CD4^+$ and $CD8^+$ macrophages, NK cells, B cells, $CD4^+CD8^+$ T cells.

The main limitation of SCH+CFA-induced EAE is the confounding influence of the adjuvant. Still, the EAE model based on immunization with SCH only is not without flaws, as there are certain common disadvantages of both models. Our results imply that irrespectively if the immunization is performed with or without CFA, CD8 T cells are not involved in EAE pathogenesis in a major way, in contrary to prominent (pahogenic and regulatory) role of this T cell subpopulation in MS (reviewed in Mockus et al., 2021). Also, the relapsing remitting course of the disease, the hallmark of MS, is not observed in all of the immunized rats. Thus, the clinical translation of the model is limited, especially for the investigation of therapeutic efficiency. Yet, this limitation can be overcome with the increase in the number of rats used in the experiments and the selection of those animals experiencing EAE relapses for the treatment. Of course, EAE induced in primates without the use of CFA might be considered as more relevant to MS due to the close phylogenetic relationship with humans (’t Hart, 2019). Still, the model described in this paper has several advantages over primate EAE. To name some: availability, lower costs of animals and their housing and maintaining, their short gestation times and genetic identity, let

alone strong political and public pressure against the use of primates in experiments. To conclude, data presented in this paper promote CFA-free SCH-induced EAE in DA rats as the preferential non-primate animal model for the studies of multiple sclerosis.

Acknowledgments

This work was supported by the Ministry of Education, Science and Technological Development, the Republic of Serbia, contract No. 451-03-9/2021-14/200007, and by the Research Group Linkage Programme of the Alexander von Humboldt Foundation, Bonn, Germany. G.K is supported by the European Research Council starting grant (GAMES; 635617), German research foundation (DFG) SFB TR-128 (Project A1), and by the Max Planck Society. The authors are thankful to Irena Lavrnja and Marija Jakovljević, Department of Neurobiology, IBISS, University of Belgrade for their assistance with histological analyses.

Conflict of interest

The authors declare that they have no conflict of interests.

References

't Hart, B.A., 2019. Experimental autoimmune encephalomyelitis in the common marmoset: a translationally relevant model for the cause and course of multiple sclerosis. Primate Biol. 6, 17–58. https://doi.org/10.5194/pb-6-17-2019

Almolda, B., Costa, M., Montoya, M., González, B., Castellano, B., 2009. CD4 microglial expression correlates with spontaneous clinical improvement in the acute Lewis rat EAE model. J. Neuroimmunol. 209, 65–80. https://doi.org/10.1016/j.jneuroim.2009.01.026

Bartholomäus, I., Kawakami, N., Odoardi, F., Schläger, C., Miljkovic, D., Ellwart, J.W., Klinkert, W.E.F., Flügel-Koch, C., Issekutz, T.B., Wekerle, H., Flügel, A., 2009. Effector T cell interactions with meningeal vascular structures in nascent autoimmune CNS lesions. Nature 462, 94–8. https://doi.org/10.1038/nature08478

Ben-Nun, A., Kaushansky, N., Kawakami, N., Krishnamoorthy, G., Berer, K., Liblau, R., Hohlfeld, R., Wekerle, H., 2014. From classic to spontaneous and humanized models of multiple sclerosis: impact on understanding pathogenesis and drug development. J. Autoimmun. 54, 33–50. https://doi.org/10.1016/j.jaut.2014.06.004

Billiau, A., Matthys, P., 2001. Modes of action of Freund's adjuvants in experimental models of autoimmune diseases. J. Leukoc. Biol. 70, 849–860.

Brooks, T.A., Hawkins, B.T., Huber, J.D., Egleton, R.D., Davis, T.P., 2005. Chronic inflammatory pain leads to increased blood-brain barrier permeability and tight junction protein alterations. Am. J. Physiol. Heart Circ. Physiol. 289, H738-43. https://doi.org/10.1152/ajpheart.01288.2004

Burrows, D.J., McGown, A., Jain, S.A., De Felice, M., Ramesh, T.M., Sharrack, B., Majid, A., 2019. Animal models of multiple sclerosis: From rodents to zebrafish. Mult. Scler. 25, 306–

324. https://doi.org/10.1177/1352458518805246

Casserly, C.S., Nantes, J.C., Whittaker Hawkins, R.F., Vallières, L., 2017. Neutrophil perversion in demyelinating autoimmune diseases: Mechanisms to medicine. Autoimmun. Rev. 16, 294–307. https://doi.org/10.1016/j.autrev.2017.01.013

Chu, Y.-C., Guan, Y., Skinner, J., Raja, S.N., Johns, R.A., Tao, Y.-X., 2005. Effect of genetic knockout or pharmacologic inhibition of neuronal nitric oxide synthase on complete Freund's adjuvant-induced persistent pain. Pain 119, 113–123. https://doi.org/10.1016/j.pain.2005.09.024

Coderre, T.J., Laferrière, A., 2020. The emergence of animal models of chronic pain and logistical and methodological issues concerning their use. J. Neural Transm. 127, 393–406. https://doi.org/10.1007/s00702-019-02103-y

Crocker, P.R., Jefferies, W.A., Clark, S.J., Chung, L.P., Gordon, S., 1987. Species heterogeneity in macrophage expression of the CD4 antigen. J. Exp. Med. 166, 613–618. https://doi.org/10.1084/jem.166.2.613

Croxford, A.L., Kurschus, F.C., Waisman, A., 2011. Mouse models for multiple sclerosis: historical facts and future implications. Biochim. Biophys. Acta 1812, 177–183. https://doi.org/10.1016/j.bbadis.2010.06.010

D'Amico, E., Zanghì, A., Gastaldi, M., Patti, F., Zappia, M., Franciotta, D., 2019. Placing CD20-targeted B cell depletion in multiple sclerosis therapeutic scenario: Present and future perspectives. Autoimmun. Rev. 18, 665–672. https://doi.org/10.1016/j.autrev.2019.05.003

Gaublomme, J.T., Yosef, N., Lee, Y., Gertner, R.S., Yang, L. V, Wu, C., Pandolfi, P.P., Mak, T., Satija, R., Shalek, A.K., Kuchroo, V.K., Park, H., Regev, A., 2015. Single-Cell Genomics Unveils Critical Regulators of Th17 Cell Pathogenicity. Cell 163, 1400–1412.

https://doi.org/10.1016/j.cell.2015.11.009

Gibbings, D., Befus, A.D., 2009. CD4 and CD8: an inside-out coreceptor model for innate immune cells. J. Leukoc. Biol. 86, 251–259. https://doi.org/10.1189/jlb.0109040

Gibbings, D.J., Marcet-Palacios, M., Sekar, Y., Ng, M.C.Y., Befus, A.D., 2007. CD8 alpha is expressed by human monocytes and enhances Fc gamma R-dependent responses. BMC Immunol. 8, 12. https://doi.org/10.1186/1471-2172-8-12

Haanstra, K.G., Jagessar, S.A., Bauchet, A.-L., Doussau, M., Fovet, C.-M., Heijmans, N., Hofman, S.O., van Lubeek-Veth, J., Bajramovic, J.J., Kap, Y.S., Laman, J.D., Touin, H., Watroba, L., Bauer, J., Lachapelle, F., Serguera, C., 't Hart, B.A., 2013. Induction of experimental autoimmune encephalomyelitis with recombinant human myelin oligodendrocyte glycoprotein in incomplete Freund's adjuvant in three non-human primate species. J. neuroimmune Pharmacol. Off. J. Soc. NeuroImmune Pharmacol. 8, 1251–1264. https://doi.org/10.1007/s11481-013-9487-z

Herbein, G., Doyle, A.G., Montaner, L.J., Gordon, S., 1995. Lipopolysaccharide (LPS) down-regulates CD4 expression in primary human macrophages through induction of endogenous tumour necrosis factor (TNF) and IL-1 beta. Clin. Exp. Immunol. 102, 430–437. https://doi.org/10.1111/j.1365-2249.1995.tb03801.x

Hiraki, K., Park, I.-K., Kohyama, K., Matsumoto, Y., 2009. Characterization of CD8-positive macrophages infiltrating the central nervous system of rats with chronic autoimmune encephalomyelitis. J. Neurosci. Res. 87, 1175–1184. https://doi.org/10.1002/jnr.21924

Hohlfeld, R., Dornmair, K., Meinl, E., Wekerle, H., 2016. The search for the target antigens of multiple sclerosis, part 2: CD8+ T cells, B cells, and antibodies in the focus of reverse-translational research. Lancet. Neurol. 15, 317–331. https://doi.org/10.1016/S1474-

4422(15)00313-0

Ibrahim, S.M., Mix, E., Böttcher, T., Koczan, D., Gold, R., Rolfs, A., Thiesen, H.J., 2001. Gene expression profiling of the nervous system in murine experimental autoimmune encephalomyelitis. Brain 124, 1927–1938. https://doi.org/10.1093/brain/124.10.1927

Jagessar, S.A., Heijmans, N., Blezer, E.L.A., Bauer, J., Blokhuis, J.H., Wubben, J.A.M., Drijfhout, J.W., van den Elsen, P.J., Laman, J.D., Hart, B.A. 't, 2012. Unravelling the T-cell-mediated autoimmune attack on CNS myelin in a new primate EAE model induced with MOG34-56 peptide in incomplete adjuvant. Eur. J. Immunol. 42, 217–227. https://doi.org/10.1002/eji.201141863

Jander, S., Lausberg, F., Stoll, G., 2001. Differential recruitment of CD8+ macrophages during Wallerian degeneration in the peripheral and central nervous system. Brain Pathol. 11, 27–38. https://doi.org/10.1111/j.1750-3639.2001.tb00378.x

Jander, S., Schroeter, M., D'Urso, D., Gillen, C., Witte, O.W., Stoll, G., 1998. Focal ischaemia of the rat brain elicits an unusual inflammatory response: early appearance of CD8+ macrophages/microglia. Eur. J. Neurosci. 10, 680–688. https://doi.org/10.1046/j.1460-9568.1998.00078.x

Jordão, M.J.C., Sankowski, R., Brendecke, S.M., Sagar, Locatelli, G., Tai, Y.-H., Tay, T.L., Schramm, E., Armbruster, S., Hagemeyer, N., Groß, O., Mai, D., Çiçek, Ö., Falk, T., Kerschensteiner, M., Grün, D., Prinz, M., 2019. Single-cell profiling identifies myeloid cell subsets with distinct fates during neuroinflammation. Science 363. https://doi.org/10.1126/science.aat7554

Kawakami, N., Nägerl, U.V., Odoardi, F., Bonhoeffer, T., Wekerle, H., Flügel, A., 2005. Live imaging of effector cell trafficking and autoantigen recognition within the unfolding

autoimmune encephalomyelitis lesion. J. Exp. Med. 201, 1805–1814. https://doi.org/10.1084/jem.20050011

Laman, J.D., Kooistra, S.M., Clausen, B.E., 2017. Reproducibility Issues: Avoiding Pitfalls in Animal Inflammation Models. Methods Mol. Biol. 1559, 1–17. https://doi.org/10.1007/978-1-4939-6786-5_1

Lavrnja, I., Smiljanic, K., Savic, D., Mladenovic-Djordjevic, A., Tesovic, K., Kanazir, S., Pekovic, S., 2017. Expression profiles of cholesterol metabolism-related genes are altered during development of experimental autoimmune encephalomyelitis in the rat spinal cord. Sci. Rep. 7, 2702. https://doi.org/10.1038/s41598-017-02638-8

Mensah-Brown, E.P., Shahin, A., Al Shamisi, M., Lukic, M.L., 2011. Early influx of macrophages determines susceptibility to experimental allergic encephalomyelitis in Dark Agouti (DA) rats. J. Neuroimmunol. 232, 68–74. https://doi.org/10.1016/j.jneuroim.2010.10.010

Miljković, D., Momčilović, M., Stanojević, Z., Rašić, D., Mostarica-Stojković, M., 2011. It is still not for the old iron: adjuvant effects of carbonyl iron in experimental autoimmune encephalomyelitis induction. J. Neurochem. 118, 205–214. https://doi.org/10.1111/j.1471-4159.2011.07303.x

Mills, K.H.G., 2011. TLR-dependent T cell activation in autoimmunity. Nat. Rev. Immunol. 11, 807–822. https://doi.org/10.1038/nri3095

Mimpen, M., Smolders, J., Hupperts, R., Damoiseaux, J., 2020. Natural killer cells in multiple sclerosis: A review. Immunol. Lett. 222, 1–11. https://doi.org/10.1016/j.imlet.2020.02.012

Mockus, T.E., Munie, A., Atkinson, J.R., Segal, B.M., 2021. Encephalitogenic and Regulatory CD8 T Cells in Multiple Sclerosis and Its Animal Models. J. Immunol. 206, 3–10.

https://doi.org/10.4049/jimmunol.2000797

Mrdjen, D., Pavlovic, A., Hartmann, F.J., Schreiner, B., Utz, S.G., Leung, B.P., Lelios, I., Heppner, F.L., Kipnis, J., Merkler, D., Greter, M., Becher, B., 2018. High-Dimensional Single-Cell Mapping of Central Nervous System Immune Cells Reveals Distinct Myeloid Subsets in Health, Aging, and Disease. Immunity 48, 599. https://doi.org/10.1016/j.immuni.2018.02.014

Namer, I.J., Steibel, J., Poulet, P., Armspach, J.P., Mohr, M., Mauss, Y., Chambron, J., 1993. Blood-brain barrier breakdown in MBP-specific T cell induced experimental allergic encephalomyelitis. A quantitative in vivo MRI study. Brain 116 (Pt 1, 147–159. https://doi.org/10.1093/brain/116.1.147

Pan, H., Guo, R., Ju, Y., Wang, Q., Zhu, J., Xie, Y., Zheng, Y., Li, T., Liu, Z., Lu, L., Li, F., Tong, B., Xiao, L., Xu, X., Leung, E.L.-H., Li, R., Yang, H., Wang, J., Zhou, H., Jia, H., Liu, L., 2019. A single bacterium restores the microbiome dysbiosis to protect bones from destruction in a rat model of rheumatoid arthritis. Microbiome 7, 107. https://doi.org/10.1186/s40168-019-0719-1

PATERSON, P.Y., BELL, J., 1962. Studies of induction of allergic encephalomyelities in rats and guinea pigs without the use of Mycobacteria. J. Immunol. 89, 72–79.

Perry, V.H., Gordon, S., 1987. Modulation of CD4 antigen on macrophages and microglia in rat brain. J. Exp. Med. 166, 1138–1143. https://doi.org/10.1084/jem.166.4.1138

Pierson, E.R., Wagner, C.A., Goverman, J.M., 2018. The contribution of neutrophils to CNS autoimmunity. Clin. Immunol. 189, 23–28. https://doi.org/10.1016/j.clim.2016.06.017

Popovich, P.G., van Rooijen, N., Hickey, W.F., Preidis, G., McGaughy, V., 2003. Hematogenous macrophages express CD8 and distribute to regions of lesion cavitation after spinal cord

injury. Exp. Neurol. 182, 275–287. https://doi.org/10.1016/s0014-4886(03)00120-1

Raghavendra, V., Tanga, F.Y., DeLeo, J.A., 2004. Complete Freunds adjuvant-induced peripheral inflammation evokes glial activation and proinflammatory cytokine expression in the CNS. Eur. J. Neurosci. 20, 467–473. https://doi.org/10.1111/j.1460-9568.2004.03514.x

Schroeter, M., Stoll, G., Weissert, R., Hartung, H.-P., Lassmann, H., Jander, S., 2003. CD8+ phagocyte recruitment in rat experimental autoimmune encephalomyelitis: association with inflammatory tissue destruction. Am. J. Pathol. 163, 1517–1524. https://doi.org/10.1016/S0002-9440(10)63508-0

Solaro, C., Trabucco, E., Messmer Uccelli, M., 2013. Pain and multiple sclerosis: pathophysiology and treatment. Curr. Neurol. Neurosci. Rep. 13, 320. https://doi.org/10.1007/s11910-012-0320-5

Sriram, S., Steiner, I., 2005. Experimental allergic encephalomyelitis: a misleading model of multiple sclerosis. Ann. Neurol. 58, 939–945. https://doi.org/10.1002/ana.20743

Stanisavljević, S., Čepić, A., Bojić, S., Veljović, K., Mihajlović, S., Đedović, N., Jevtić, B., Momčilović, M., Lazarević, M., Mostarica Stojković, M., Miljković, Đ., Golić, N., 2019. Oral neonatal antibiotic treatment perturbs gut microbiota and aggravates central nervous system autoimmunity in Dark Agouti rats. Sci. Rep. 9, 918. https://doi.org/10.1038/s41598-018-37505-7

Stosic-Grujicic, S., Ramic, Z., Bumbasirevic, V., Harhaji, L., Mostarica-Stojkovic, M., 2004. Induction of experimental autoimmune encephalomyelitis in Dark Agouti rats without adjuvant. Clin. Exp. Immunol. 136, 49–55. https://doi.org/10.1111/j.1365-2249.2004.02418.x

Tutaj, M., Szczepanik, M., 2007. Epicutaneous (EC) immunization with myelin basic protein (MBP) induces TCRalphabeta+ CD4+ CD8+ double positive suppressor cells that protect from experimental autoimmune encephalomyelitis (EAE). J. Autoimmun. 28, 208–215. https://doi.org/10.1016/j.jaut.2007.02.017

van den Hoogen, W.J., Laman, J.D., 't Hart, B.A., 2017. Modulation of Multiple Sclerosis and Its Animal Model Experimental Autoimmune Encephalomyelitis by Food and Gut Microbiota. Front. Immunol. 8, 1081. https://doi.org/10.3389/fimmu.2017.01081

Wildner, G., 2019. Are rats more human than mice? Immunobiology 224, 172–176. https://doi.org/10.1016/j.imbio.2018.09.002

Wu, J., Zhou, C., Robertson, J., Carlock, C., Lou, Y.-H., 2014. Peripheral blood CD8αα+CD11c+MHC-II+CD3- cells attenuate autoimmune glomerulonephritis in rats. Kidney Int. 85, 1078–1090. https://doi.org/10.1038/ki.2013.456

Zhang, Z.-M., Shi, R., Chen, H., Zhang, Z., 2016. Lesional accumulation of CD8(+) cells in sciatic nerves of experimental autoimmune neuritis rats. Neurol. Sci. Off. J. Ital. Neurol. Soc. Ital. Soc. Clin. Neurophysiol. 37, 199–203. https://doi.org/10.1007/s10072-015-2384-x

Figure legends

Fig 1. Comparison of EAE in SCH- and SCH+CFA-immunized DA rats. Clinical signs of EAE in female (n=11) and male (n=12) DA rats immunized with SCH (A). Clinical signs of EAE in DA rats immunized with SCH (n=42) or with SCH+CFA (n=39) (B). Representative photomicrographs of spinal cord lesions (C), the number of infiltrates per section (n=120) of the spinal cord tissue (D), the number of cells per infiltrate (E), and representative photomicrographs of spinal cord sections stained with Sudan Black (F). d.p.i. – day post-immunization. Scale bars are set to 500 μm. Arrowhead indicates mononuclear cell infiltrate. Arrow indicates demyelination. Data are presented as mean + SEM. *p<0.05 SCH *vs.* SCH+CFA

Fig 2. Phenotype of lymph node cells of SCH- and SCH+CFA-immunized DA rats. Popliteal and inguinal lymph nodes were isolated from non-immunized DA rats (non-imm). Popliteal lymph nodes were isolated from DA rats immunized with SCH or with SCH+CFA at 4 and 6 d.p.i. The proportion and number of cells expressing the markers of interest are presented (A-AE). Data from 5 rats are presented as mean + SD. $^{\#}$p<0.05 *vs.* non-imm, *p<0.05 SCH *vs.* SCH+CFA

Fig 3. MBP-stimulated IFN-γ and IL-17 production in lymph node cells. Popliteal lymph nodes were isolated from SCH- and SCH+CFA-immunized DA rats at 6 d.p.i. Lymph node cells were stimulated with MBP for 24h and IL-17 (A) and IFN-γ (B) cytokine levels in cell culture supernatants were determined by ELISA. Data from 5 rats are presented as mean + SD. *p<0.05 SCH *vs.* SCH+CFA; $^{\#}$ p<0.05 0 *vs.* MBP

Fig 4. Phenotype of spinal cord immune cells of SCH- and SCH+CFA-immunized DA rats. Spinal cords were dissected from DA rats immunized with SCH or SCH+CFA at the peak of EAE. Immune cells were isolated from the spinal cords and analyzed phenotypically by cytofluorimetry. The number of cells (A) and the proportion of cells expressing the markers of interest are presented (B-G). Data from 5 rats are presented as mean + SD. *$p<0.05$ SCH *vs.* SCH+CFA

Fig 5. Phenotype of spinal cord immune cells during EAE in SCH-immunized DA rats. Spinal cords were dissected from DA rats immunized with SCH at the onset, peak, and recovery phase of EAE. Immune cells were isolated from the spinal cords and analyzed phenotypically by cytofluorimetry. The number of cells (A), the proportion of cells expressing the markers of interest (B-I, K, L), and the mean fluorescence intensity (MFI) of MHCII expression on antigen-presenting cells (J, M) are presented. Data from 5 rats are presented as mean + SD. *$p<0.05$ *vs.* onset; $^{\#}p<0.05$ *vs.* peak

Supplementary Fig 1. Representative gating strategies for cytofluorimetry. Cells were gated to live cells (gate R1 based on FSC/SSC) and cell doublets were excluded (gate R2 for singlets based on FSC/FSC-W). All the analyses were performed on cells belonging to both R1 and R2.

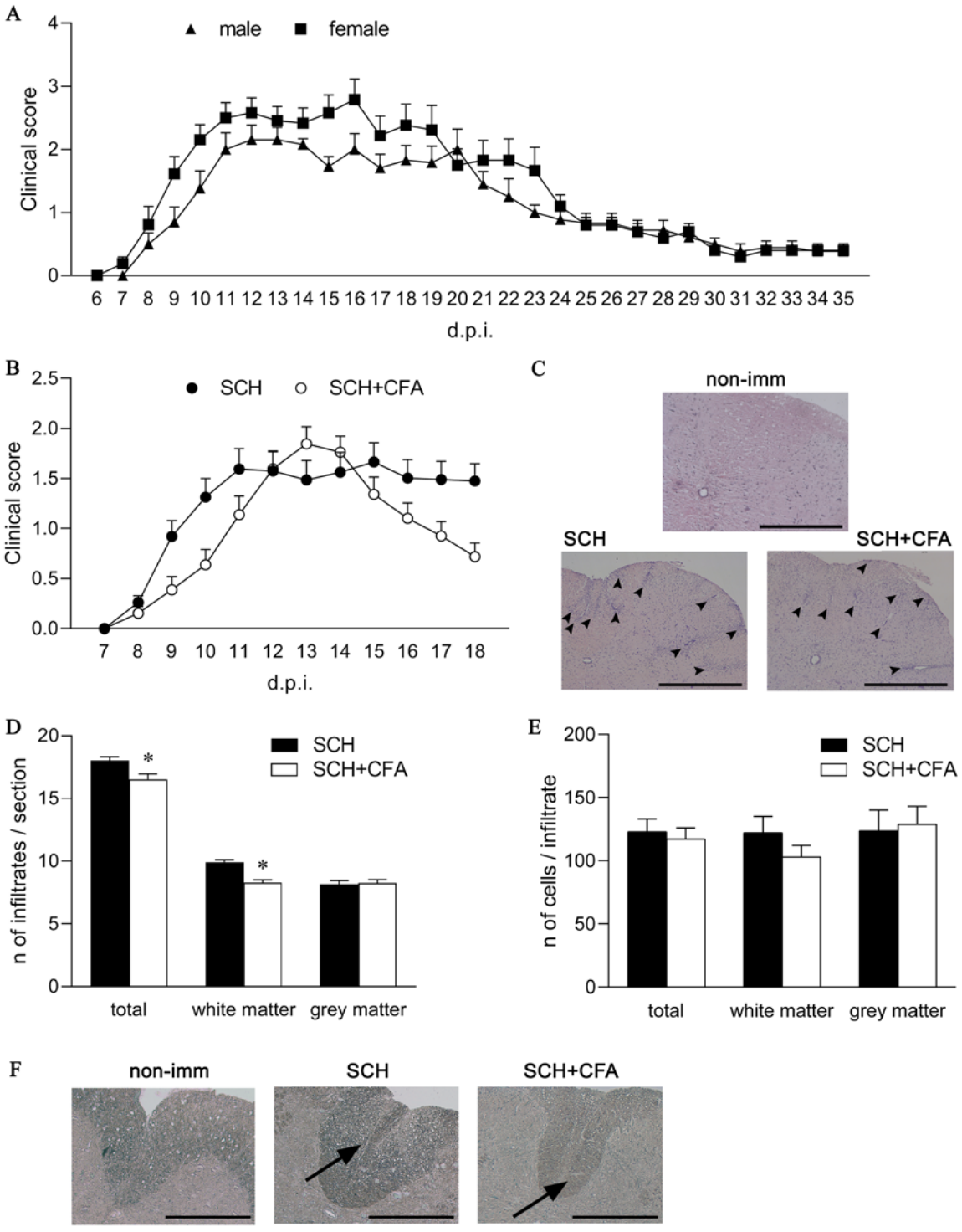
A
male
female
Clinical score
d.p.i.
B
SCH
SCH+CFA
Clinical score
d.p.i.
C
non-imm
SCH
SCH+CFA
D
SCH
SCH+CFA
n of infiltrates / section
total
white matter
grey matter
E
SCH
SCH+CFA
n of cells / infiltrate
total
white matter
grey matter
F
non-imm
SCH
SCH+CFA

Fig. 1.

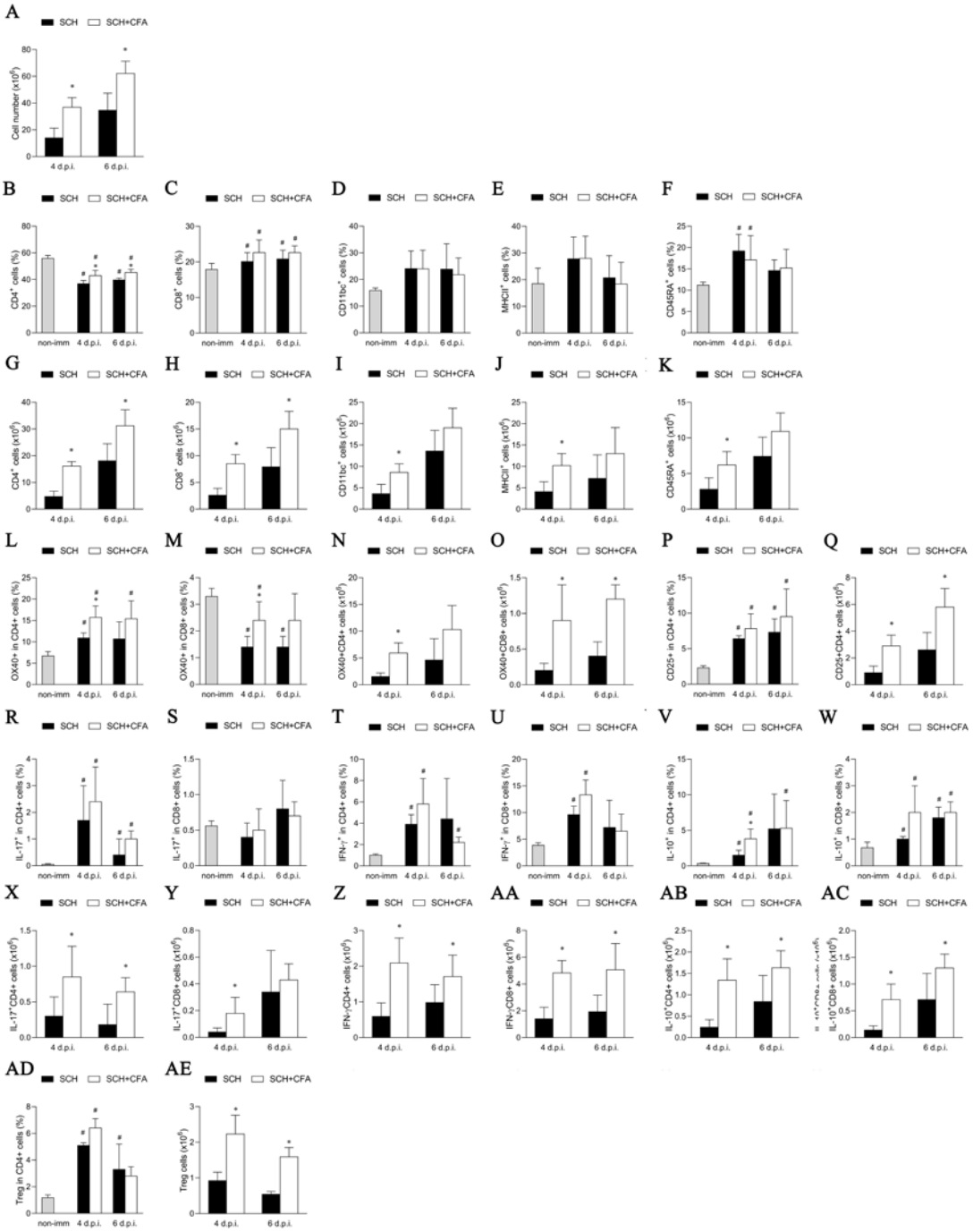
A
SCH
SCH+CFA
Cell number (x10⁶)
4 d.p.i.
6 d.p.i.
B
CD4⁺ cells (%)
C
CD8⁺ cells (%)
D
CD11bc⁺ cells (%)
E
MHCII⁺ cells (%)
F
CD45RA⁺ cells (%)
non-imm
G
CD4⁺ cells (x10⁶)
H
CD8⁺ cells (x10⁶)
I
CD11bc⁺ cells (x10⁶)
J
MHCII⁺ cells (x10⁶)
K
CD45RA⁺ cells (x10⁶)
L
OX40+ in CD4+ cells (%)
M
OX40+ in CD8+ cells (%)
N
OX40+CD4+ cells (x10⁶)
O
OX40+CD8+ cells (x10⁶)
P
CD25+ in CD4+ cells (%)
Q
CD25+CD4+ cells (x10⁶)
R
IL-17⁺ in CD4+ cells (%)
S
IL-17⁺ in CD8+ cells (%)
T
IFN-γ⁺ in CD4+ cells (%)
U
IFN-γ⁺ in CD8+ cells (%)
V
IL-10⁺ in CD4+ cells (%)
W
IL-10⁺ in CD8+ cells (%)
X
IL-17⁺CD4+ cells (x10⁶)
Y
IL-17⁺CD8+ cells (x10⁶)
Z
IFN-γ⁺CD4+ cells (x10⁶)
AA
IFN-γ⁺CD8+ cells (x10⁶)
AB
IL-10⁺CD4+ cells (x10⁶)
AC
IL-10⁺CD8+ cells (x10⁶)
AD
Treg in CD4+ cells (%)
AE
Treg cells (x10⁶)

Fig. 2.

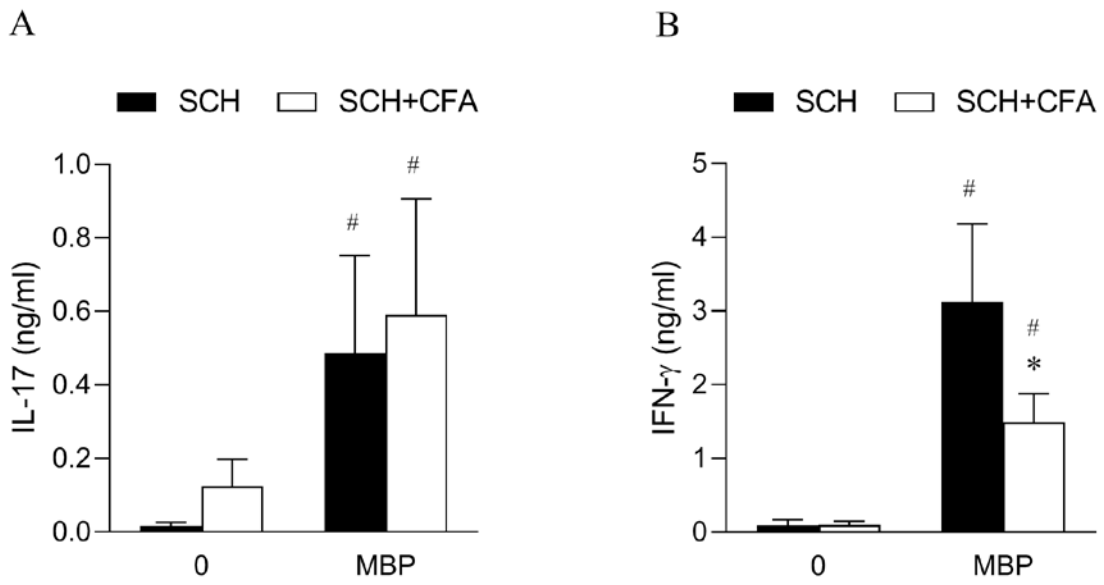
A
SCH
SCH+CFA
IL-17 (ng/ml)
1.0
0.8
0.6
0.4
0.2
0.0
#
#
0
MBP
B
SCH
SCH+CFA
IFN-γ (ng/ml)
5
4
3
2
1
0
#
#
*
0
MBP

Fig. 3

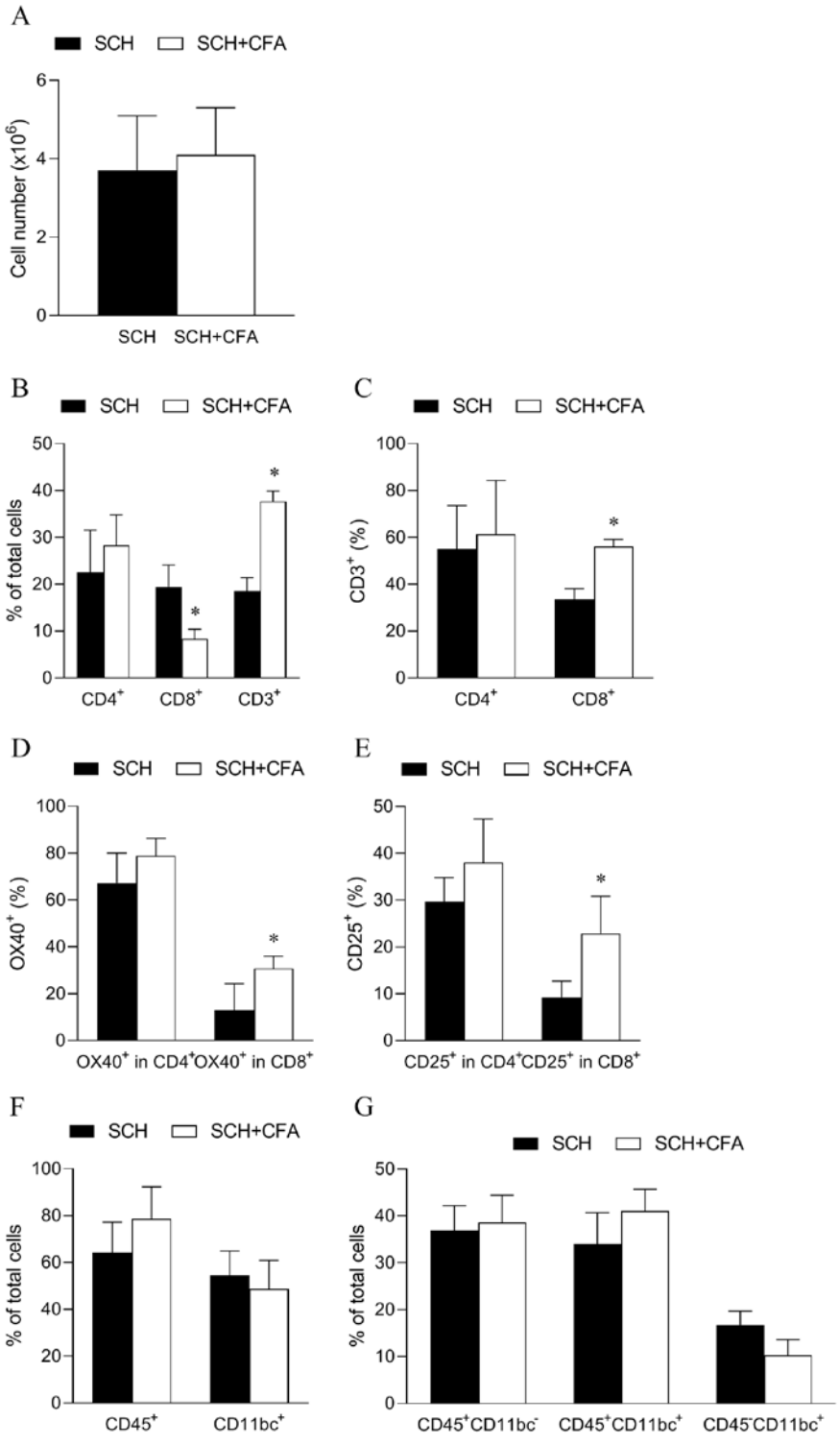
A
SCH
SCH+CFA
Cell number (x10^6)
SCH
SCH+CFA
B
% of total cells
CD4+
CD8+
CD3+
C
CD3+ (%)
CD4+
CD8+
D
OX40+ (%)
OX40+ in CD4+
OX40+ in CD8+
E
CD25+ (%)
CD25+ in CD4+
CD25+ in CD8+
F
% of total cells
CD45+
CD11bc+
G
% of total cells
CD45+CD11bc-
CD45+CD11bc+
CD45-CD11bc+

Fig. 4

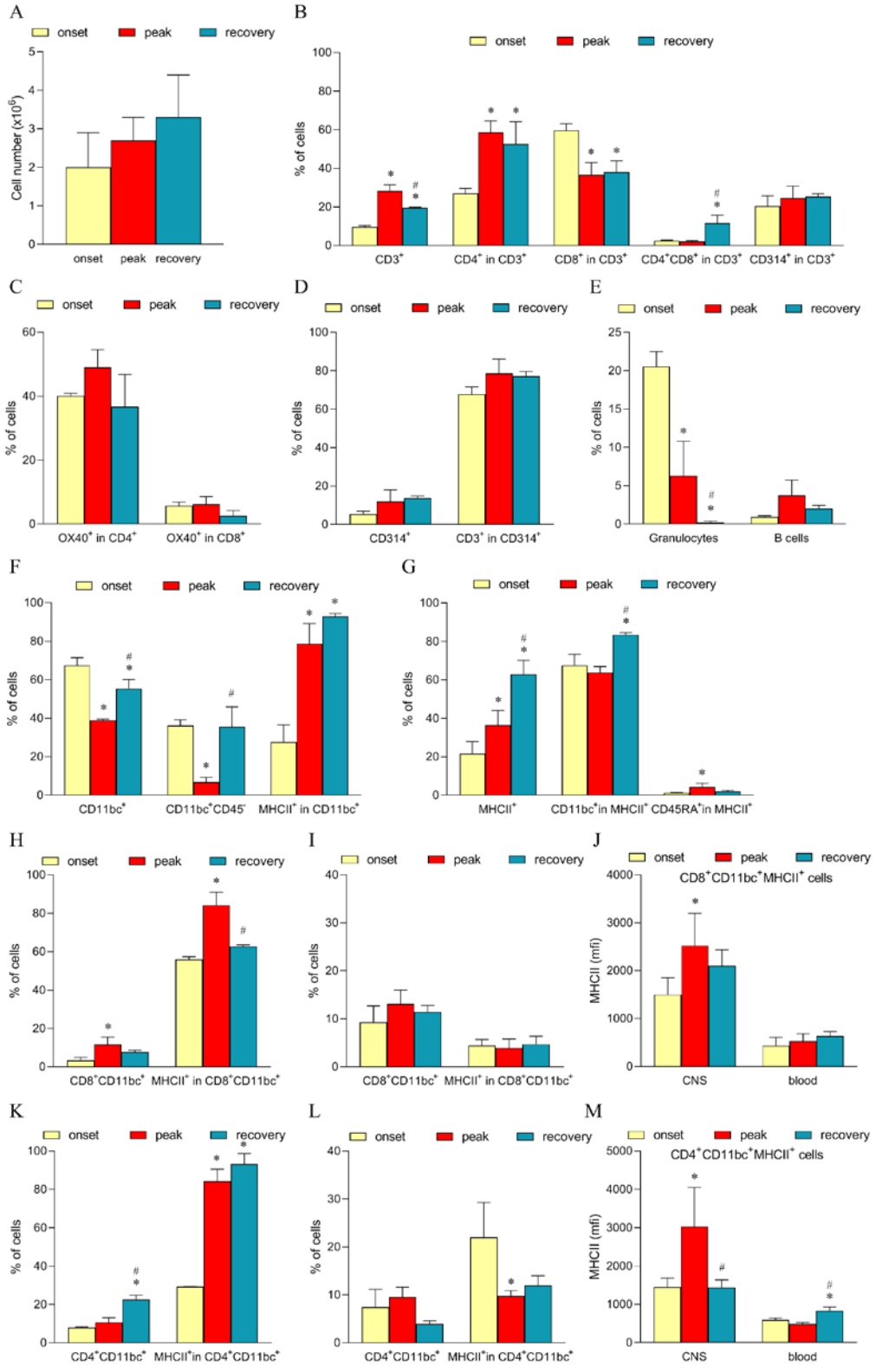
A
onset
peak
recovery
Cell number (x10^6)
onset peak recovery
B
% of cells
CD3+
CD4+ in CD3+
CD8+ in CD3+
CD4+CD8+ in CD3+
CD314+ in CD3+
C
OX40+ in CD4+
OX40+ in CD8+
D
CD314+
CD3+ in CD314+
E
Granulocytes
B cells
F
CD11bc+
CD11bc+CD45-
MHCII+ in CD11bc+
G
MHCII+
CD11bc+in MHCII+ CD45RA+in MHCII+
H
CD8+CD11bc+
MHCII+ in CD8+CD11bc+
I
J
CD8+CD11bc+MHCII+ cells
MHCII (mfi)
CNS
blood
K
CD4+CD11bc+
MHCII+in CD4+CD11bc+
L
M
CD4+CD11bc+MHCII+ cells

Fig. 5

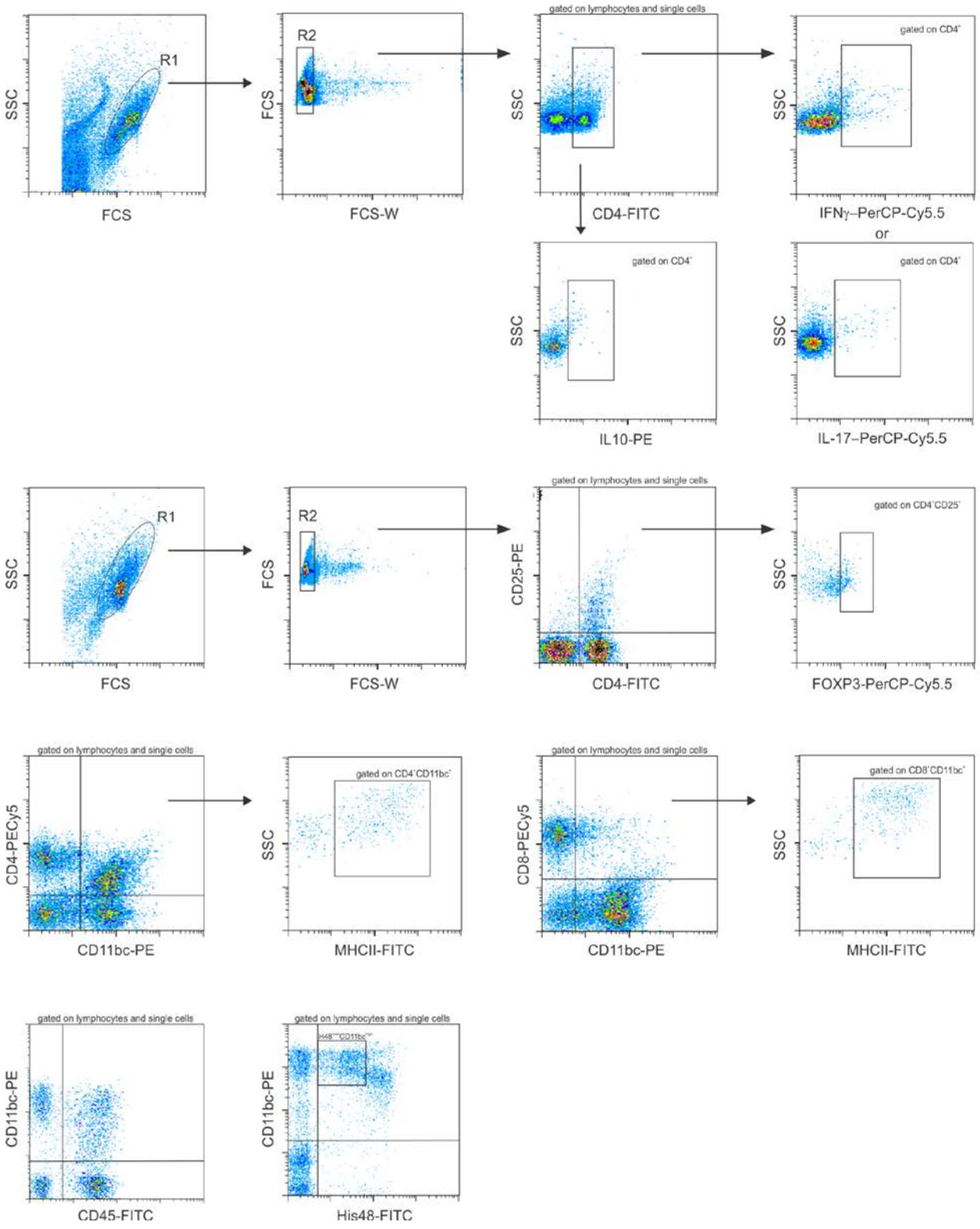
R1
SSC
FCS
R2
FCS
FCS-W
gated on lymphocytes and single cells
SSC
CD4-FITC
gated on CD4+
SSC
IFNγ–PerCP-Cy5.5
or
gated on CD4+
SSC
IL10-PE
gated on CD4+
SSC
IL-17–PerCP-Cy5.5
R1
SSC
FCS
R2
FCS
FCS-W
gated on lymphocytes and single cells
CD25-PE
CD4-FITC
gated on CD4+CD25+
SSC
FOXP3-PerCP-Cy5.5
gated on lymphocytes and single cells
CD4-PECy5
CD11bc-PE
gated on CD4+CD11bc+
SSC
MHCII-FITC
gated on lymphocytes and single cells
CD8-PECy5
CD11bc-PE
gated on CD8+CD11bc+
SSC
MHCII-FITC
gated on lymphocytes and single cells
CD11bc-PE
CD45-FITC
gated on lymphocytes and single cells
CD11bc-PE
His48-FITC

Suppl. Fig. 1